Chapter 5

Shared-Aperture Multi-Band Dual-Polarized SAR Microstrip Array Design

Shun-Shi Zhong and Zhu Sun

Additional information is available at the end of the chapter

http://dx.doi.org/10.5772/54666

1. Introduction

Since the 1970s, the remote sensing synthetic aperture radar (SAR) systems have been developing increasingly. The SIR-C/X SAR mounted on the American Space Shuttle Endeavour firstly completed the high resolution 3D imaging all over the globe in Feb. 2000 [1]. It employs three dual-polarized sub-arrays operating at L-, C- and X-bands, respectively, as shown in Fig. 1[2]. The multi-band dual-polarized array receives more target information than that of a single-band one-polarization counterpart, and thus enhances the capability of target detection and identification. The common bands of space-borne SARs are L (center at 1.275 GHz), S (3.0 GHz), C (5.3 GHz) and X (9.6 GHz) bands. To minimize the volume and weight of a SAR antenna, a common aperture configuration for dual or multiple bands are expected, which will share the sub-systems behind the array as well. As a result, a lot of shared-aperture dual-band dual-polarization (DBDP) integrated planar antennas have been proposed in the last two decades [2].

The typical configurations of the shared-aperture DBDP planar arrays include the perforated structure, the interlaced layout and the overlapped layout. The perforated structure mainly includes perforated-patch/patch [3,4], ring/patch [5-7] and cross-patch/patch[8]. The interlaced layout includes interlace patch with dipole/slot [9-11] and interlaced slot with slot/dipole [12-13], *etc*. [14-15] present the review and comparison for these arrays. Both the perforated structure and interlaced layout are commonly adopted in space- or air-borne applications because of their low profile performance. On the other hand, the overlapped layout can provide further improvement in the bandwidths of dual bands, but with larger antenna profile. In [16], the thick air layer and an L-probe feed are applied to design a dual-band element of overlapped layout and a wide bandwidth is achieved at both low and high bands. Meanwhile, in the element aspect, some shapes [17-18] and a considerable number of feed methods, such as

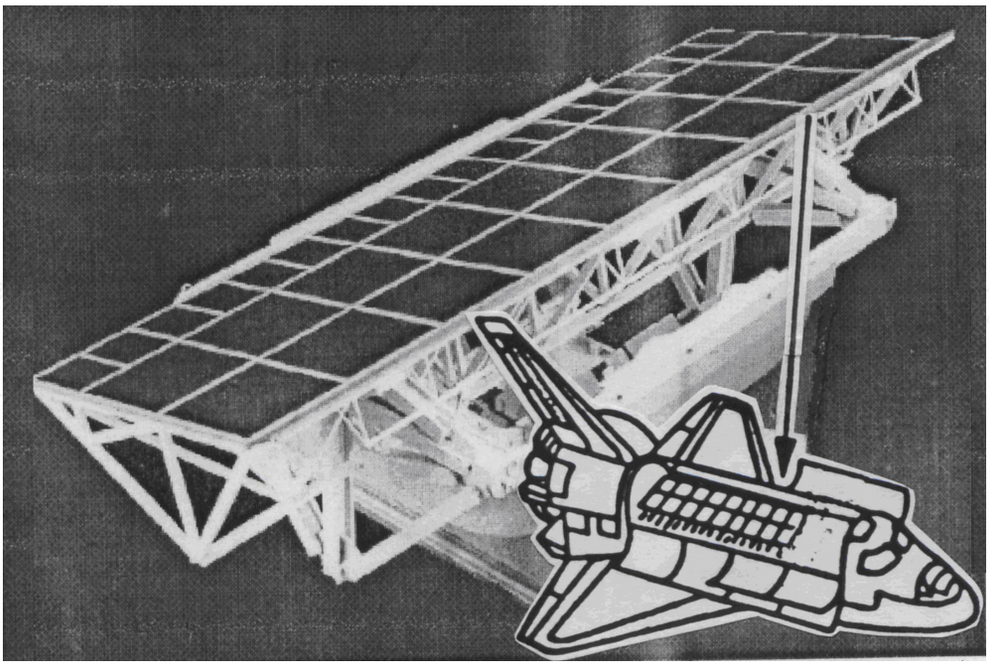

Figure 1. Antenna of SIR-C/X SAR

probe-feed [19], aperture-coupled [17-18], proximity-coupled [20], and L-shape feed [21] are proposed to improve the key performances. Besides, balanced-feed [22, 23] and hybrid-feed [24-27] are also proposed to enhance the port isolation or cross-polarization performance. Recently, a DBDP array with an impressive $S_{11} \leq -15$ dB bandwidth of 8% in the low band is introduced by using the feed skills above mentioned [28].

In this chapter a universal multi-band SAR array synthetic method is introduced to extend the shared-aperture DBDP array to a shared-aperture MBDP SAR array. As a validation, a shared-aperture L/S/X tri-band dual-polarized (TBDP) array prototype was fabricated and measured with the central frequencies of 1.25 GHz, 3.5 GHz, and 10 GHz for L-, S- and X- bands, respectively [29]. The array design and measured results are presented and discussed.

2. Array configuration

2.1. TBDP array configuration

From the system view, a similar beamwidth in the transverse (elevation) direction for each band is desired, which means that the transverse dimension of aperture for each band should be in proportion to its wavelength [3]. As an example, the transverse dimensions of aperture in L-, S- and X- bands for the SIR-C/X-SAR are 2.95 m, 0.75 m, and 0.4 m, respectively, which have the ratio of 7.375:1.875:1. Then for a TBDP array with three independent apertures of L/S/X bands, its corresponding transverse dimension of aperture may be 2.88 m for L-band, 1.08 m for S-band and 0.36 m for X-band with the ratio of 8:3:1, as seen in Fig.2a.

http://dx.doi.org/10.5772/54666

In this chapter a novel design method is proposed, as shown in Fig.2b, where L/S and L/X sub-arrays are set on the two sides, and L-band sub-array is located in the middle. Then the transverse dimensions of aperture is 1.08+1.44+0.36 =2.88m for L-band, 1.08 m for S-band and 0.36 m for X-band, with ratio of 8:3:1 that is close to the central wavelength ratio of L-, S- and X-bands. Thus S-band and X-band elements are physically separated by a large spacing to avoid mutual interference, and a 33% off in aperture size is achieved as compared to its counterpart with independent tri-band aperture of 1.08 + 2.88 + 0.36 = 4.32 m. Actually, this method divides a TBDP shared-aperture array into two DBDP shared-aperture sub-arrays and one single-band DP sub-array so that the foregone works of DBDP shared-aperture arrays can be consulted and eventually the development of a TBDP shared-aperture array will be simplified.

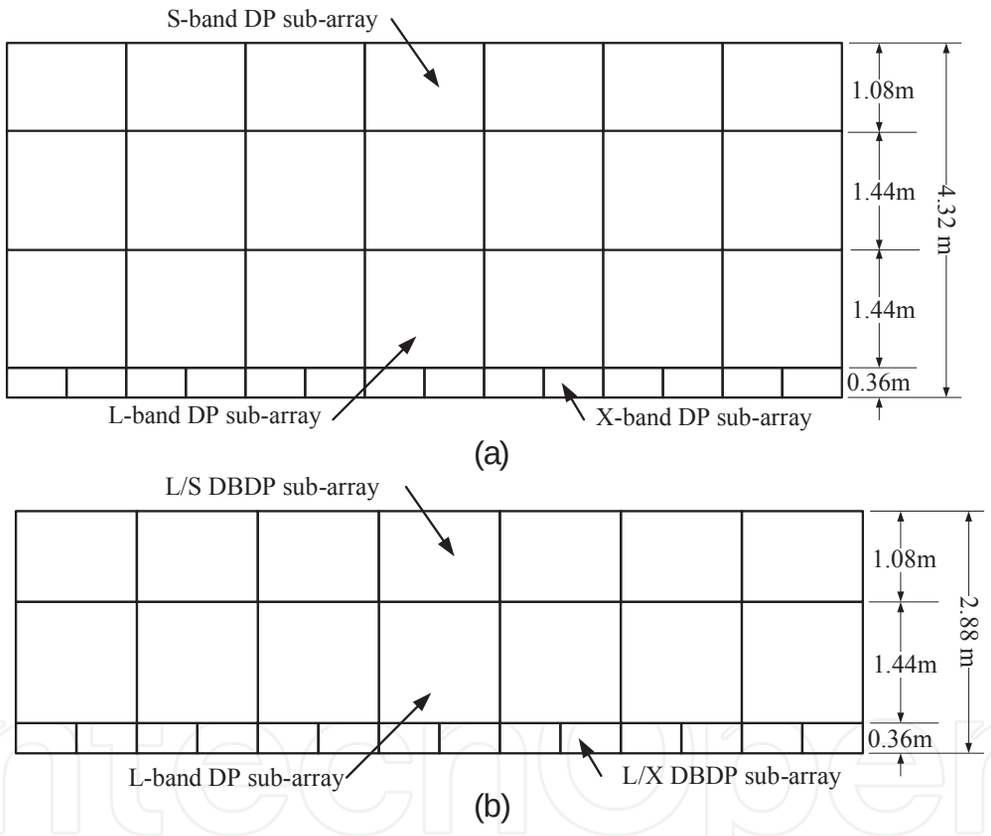

Figure 2. TBDP array configuration

2.2. L/S, L/X & L sub-array configuration

The interlaced configuration of Fig.3 is adopted for the L/S and L/X DBDP shared-aperture sub-array designs, which is more flexible for the odd frequency ratio than the perforated one[10]. Moreover, the "pair-wise anti-phase feeding" technique [30] is used in both S- and X-bands to improve the cross-polarization performance and the polarization isolation of whole array as well.

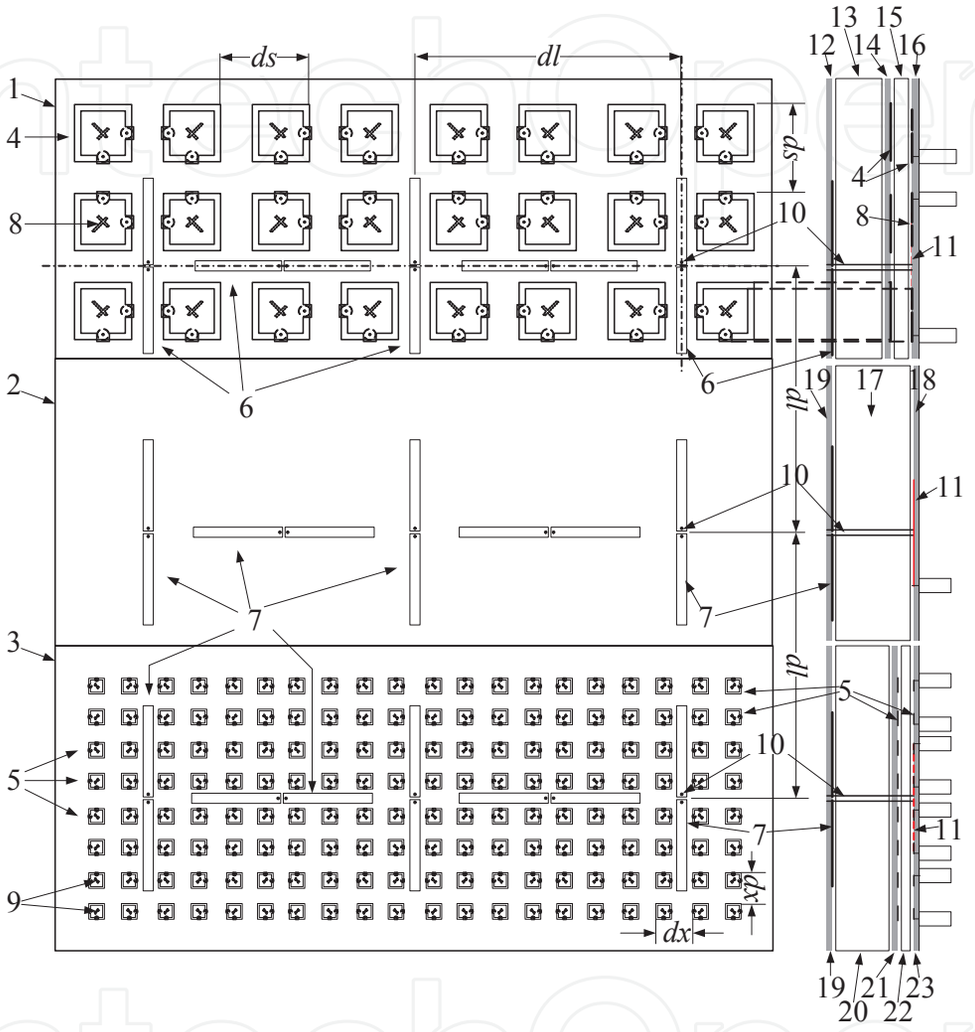

1 L/S DBDP sub-array 2 L band DP sub-array 3 L/X DBDP sub-array 4 S band stacked patch
5 X band stacked patch 6 L band print dipole (L/S) 7 L band print dipole (L/X & L)
8 isolation-slot etached on driven patch (S-band) 9 isolation-slot etached on driven patch (X-band)
10 Two-wire feeder 11 Balun of L-band 12/14/16/18/19/21/21 Substrate (Rogers 6002)
13/15/17/20/22 Foam

Figure 3. TBDP array configuration

The S-band and X-band elements in L/S and L/X DBDP arrays are distributed in square lattices, with the element spacing of $0.65\ \lambda_0$ at X-band and $0.62\ \lambda_0$ at S-band for convenience in the integration and satisfying the requirement of scanning capability (± 25°). In the L/S, L/X and L sub-arrays, the same L-band element is used to keep uniform radiation characteristic and S

http://dx.doi.org/10.5772/54666

parameters. Besides, on the purpose of realizing dual polarization as well as enhancing the polarization isolation, "T"-shaped orthogonal-set microstrip dipoles are applied. Since that the phase centers for H- and V- polarization will deviate from each other as the "T"-shaped configuration is adopted, to ensure the superposition of the phase centers for H- and V-polarization, one more vertical microstrip dipole is added in the array prototype. This makes a little difference in the beamwidths of H- and V- polarization, however, this may not be a problem when the array aperture becomes larger, which is the case for most space-borne SAR antennas, e.g. the lengthwise aperture dimension of the SIR-C/X-SAR for all three bands is 12 m.

Since this is a phased array with two-dimensional scanning capability, each element is terminated to a T/R module and a beam controller is employed to steer the beam rather than a fixed feed network. Thus final output of each element is connected to a SMA connector.

3. Element design

3.1. S- & X-band element

To meet the requirements of bandwidth and cross-polarization as well as to simplify the design and fabrication, stacked patches are adopted for the S-band (in L/S sub-array) and X-band (in L/X sub-array) elements. To realize the dual-polarized radiation, the element should be symmetric in two dimensions, so that circular and square (rectangular) shapes are the most common ones. In this design, the square patch is adopted for its better cross-polarization performance [27] and lower fabrication tolerance, as shown in Fig.4.

The feeding approach greatly refers to the isolation and the cross-polarization level of an element. [17, 21] have presented profound studies on the feeding technique of stacked patches. In [26], the excellent isolation of better than 40dB is measured by using the hybrid excitation and a balanced feed. As the cost, however, these feeding approaches are too complicated as they are applied to the array environment, because that the aperture coupling and the balanced feed are difficult for the vertical connection, while the balanced feed needs a 180 degree feed network. To ensure the fabrication reliability, the dual-probe feed is finally employed, although its isolation is not as good as the aforementioned methods.

To overcome this drawback, an asymmetric slot is etched on the driven patch to improve the port isolation [31]. Fig.5 and Fig.6 are the calculated S parameters and radiation patterns simulated by HFSS 10.0, showing the change of isolation and cross-polarization with the slot loaded. Different slot shapes are used for the S- and X- band driven patches to improve the isolation. In addition, it is found that the "H"-shaped slot in Fig.4b has less impact to S_{11} than the "cross"-shaped slot in Fig.4a, thus one has to rematch the element of latter while the "H"-shaped needs not. As seen from Fig.7, the field disturbance introduced by the slot deteriorates the element cross-polarization level. Fortunately, this would not be a problem for an array as the "pair-wise anti-phase feed" technique is used in the array configuration. The detailed design of the S/X stacked patches has been introduced in [32].

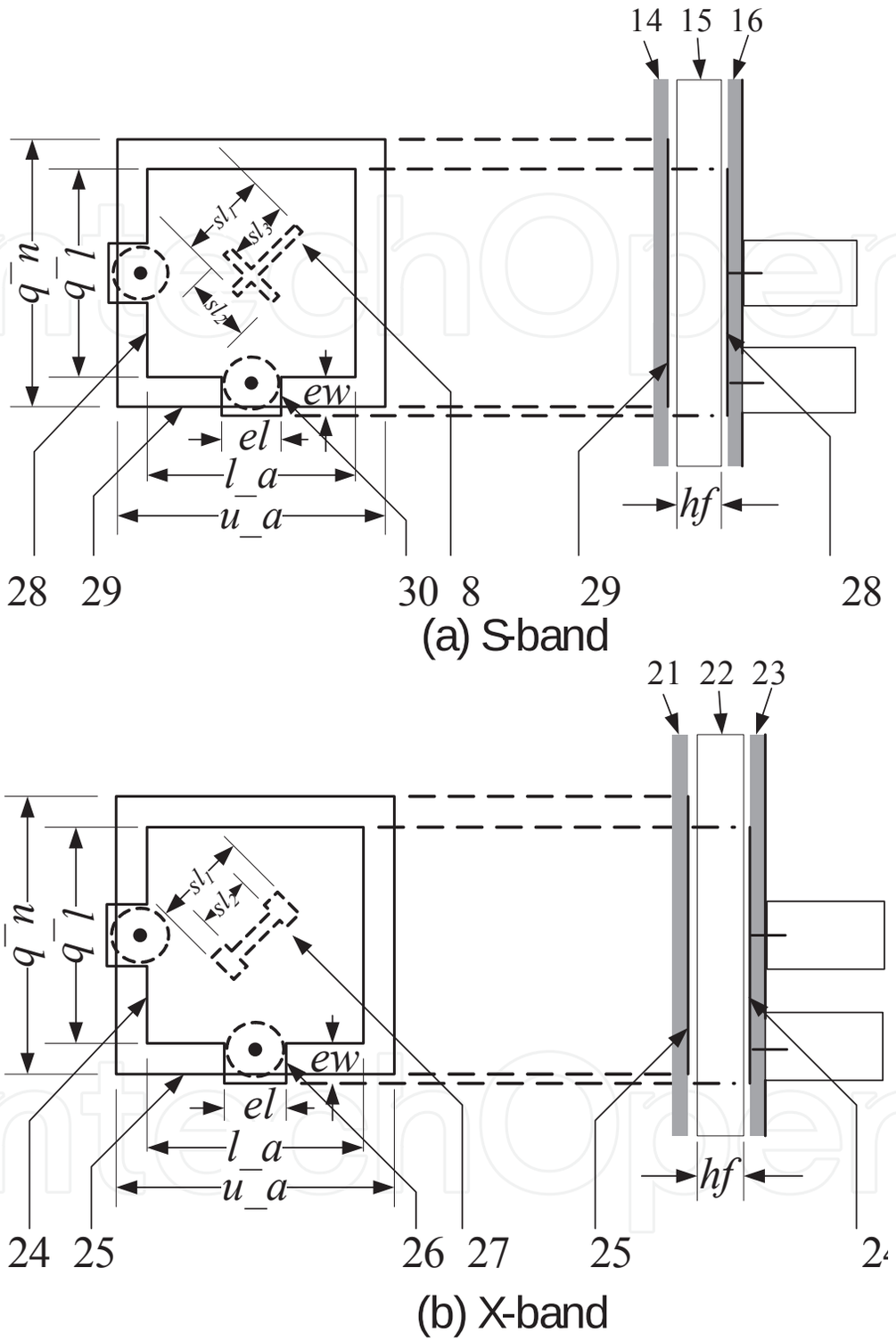

14/16 Substrate (Rogers 6002) 15 Foam 8 Isolation-slot etched on driven patch
28 Driven patch 29 Parasitic patch 30 Probe feed
21/23 Substrate (Rogers 6002) 22 Foam 24 Driven patch
25 Parasitic patch 26 Feed point 27 Isolation-slot etched on driven patch

Figure 4. S-and X-band stacked patches with slot etched

http://dx.doi.org/10.5772/54666

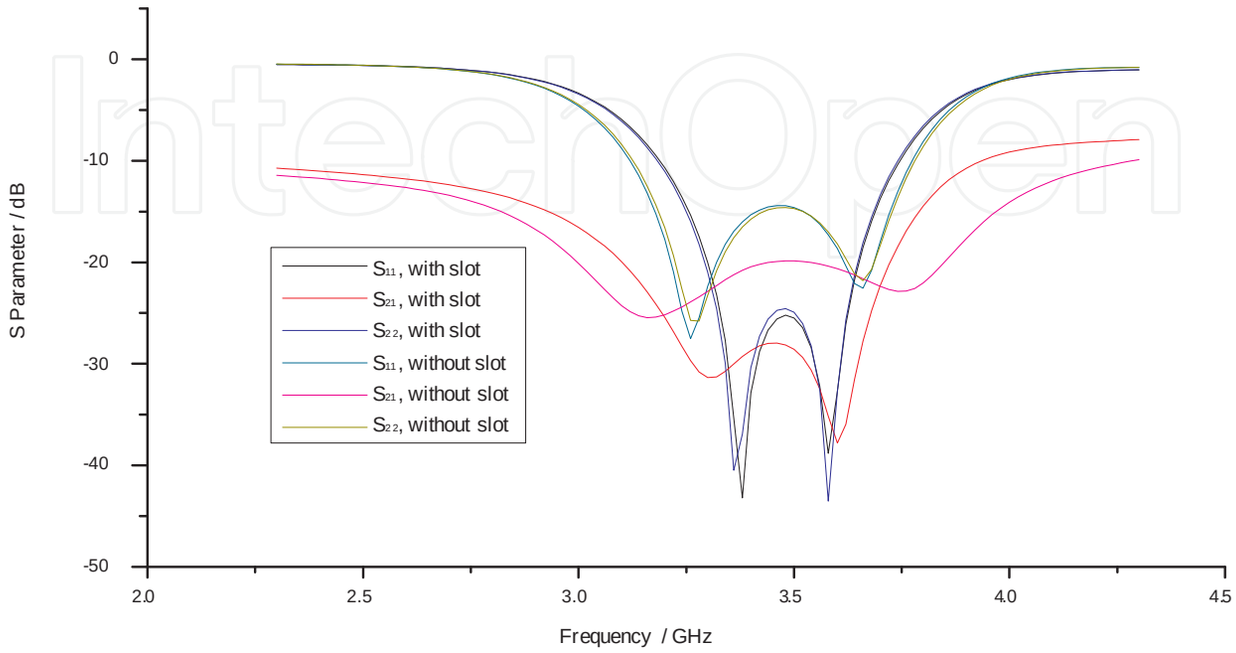

(a) S-band

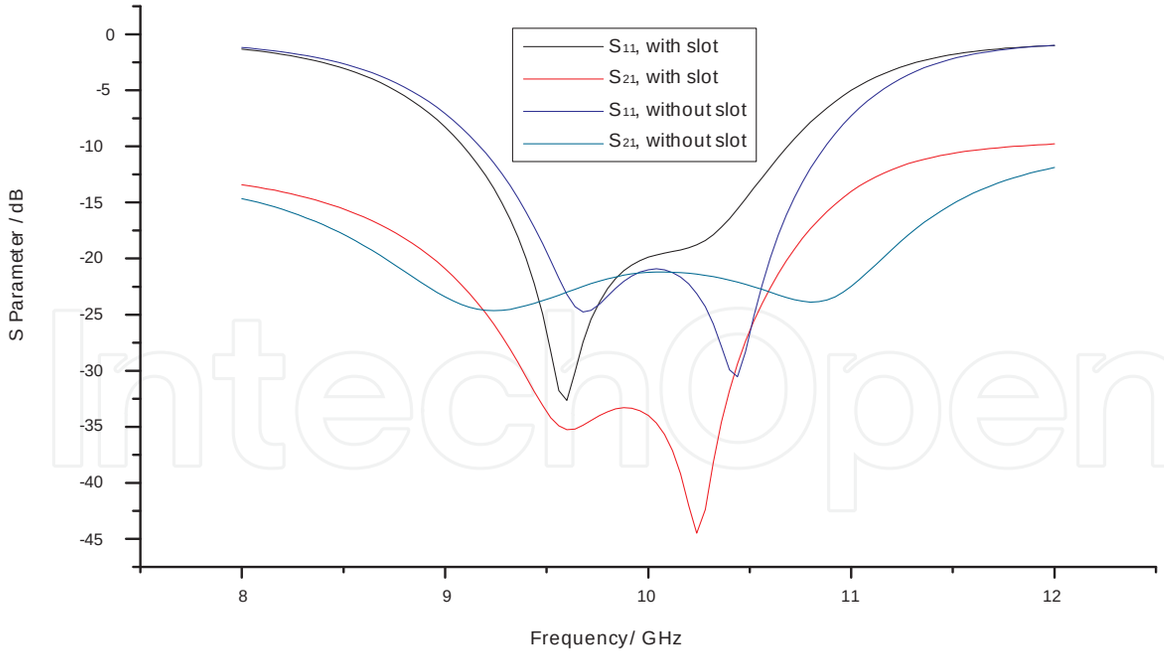

(b) X-band

Figure 5. Isolation improvement of slot-loaded stacked patches

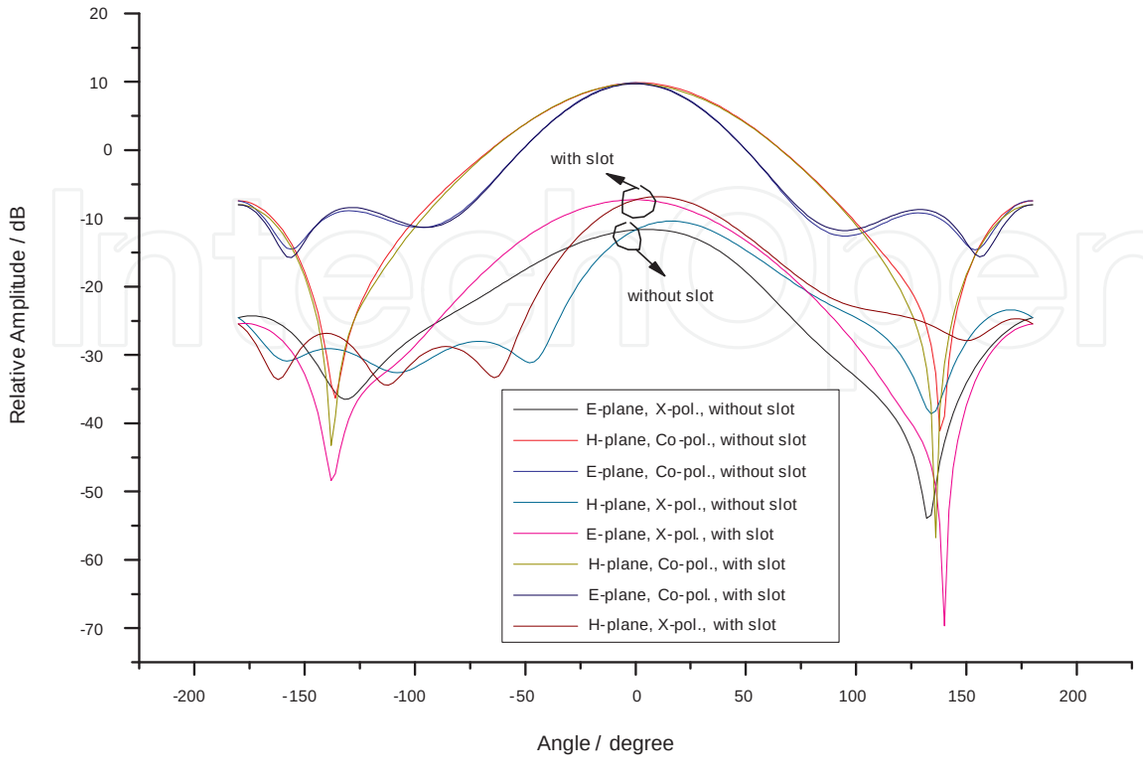

(a) S-band

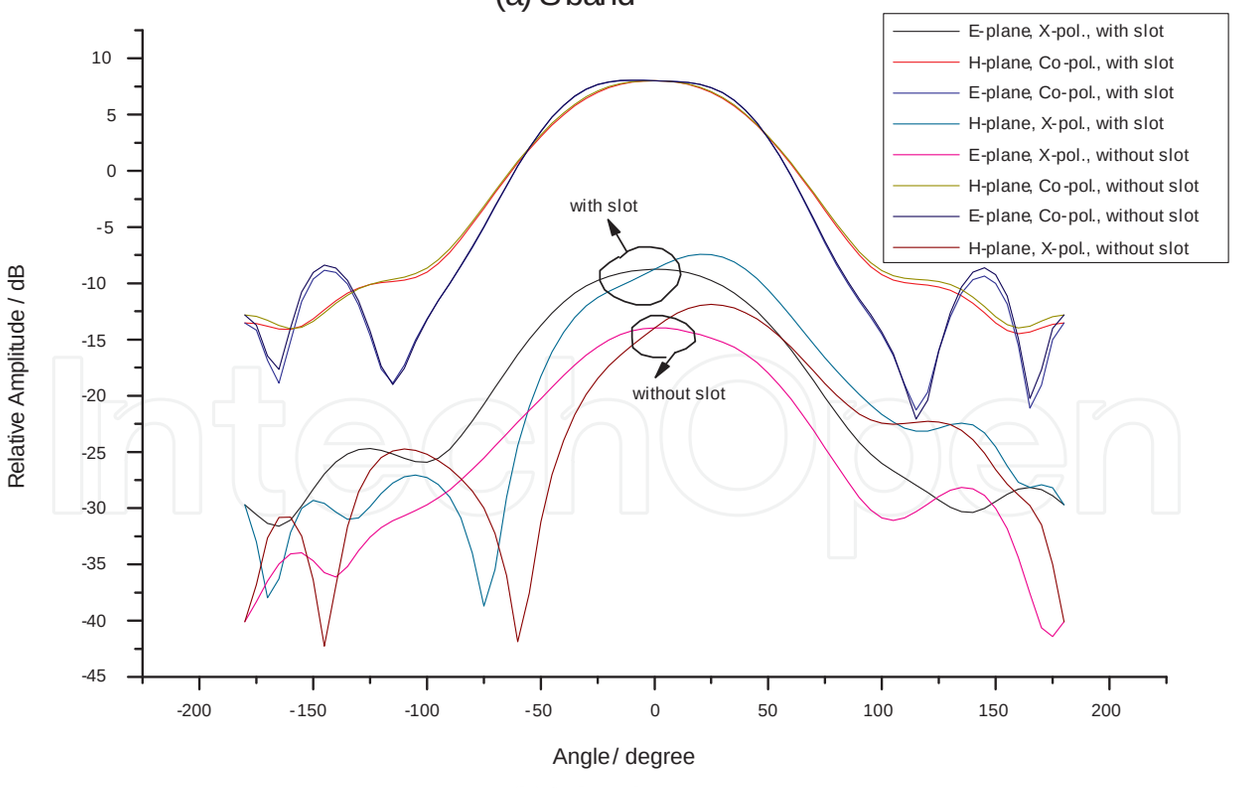

(b) X-band

Figure 6. Radiation patterns of slot-loaded elements

http://dx.doi.org/10.5772/54666

3.2. L-band element

For L/S, L/X and L sub-arrays, the structure of L-band microstrip dipole is almost the same. The only difference is the length of L-band dipole in L/S sub-array, which is shortened by 20% than its counterparts in L/X and L sub-arrays. In order to avoid the conflicting in sub-array splitting caused by the odd frequency ratio of about 3:1 for L- to S-band, the capacities are intentionally introduced in its feed network to realize a minimized design (See Fig.4).

The structure of L-band dipole is detailed in Fig.6. The microstrip dipole is printed on the top layer with a height of $\lambda_0/4$ above the ground, while the ground, in this case, serves as a reflecting metal plate. An microstrip feed network is designed to generate 180 degree phase shift, and then it is vertically transferred to a parallel two-wire line, finally this line connects to the microstrip dipole. In addition, an open-ended microstrip stub is adopted at the exciting point to realize the impedance match.

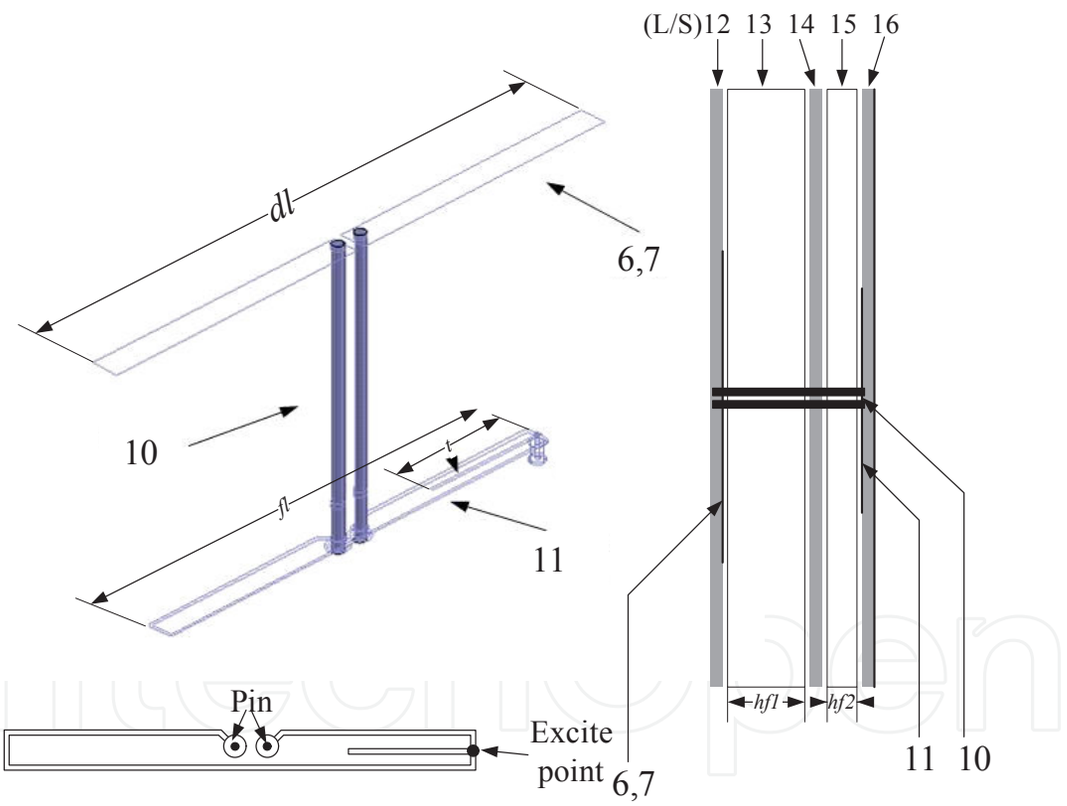

6/7 Printed dipole 10 Two-wire feeder 11 180 degree phase shifter 12/14/16 Substrate 13/15 Foam (Rogers 6002)

Figure 7. L-band microstrip dipole

This element as well as its feed structure is very slim and thus can be flexibly interlaced in the gap of S- and X-band elements. Although the profile of L-band element is somewhat high, its intrinsic broadband and good cross-polarization performance make it suitable for the TBDP SAR antenna mission.

4. Measurement results

A shared-aperture L/S/X TBDP array prototype was fabricated and measured to validate the design. Figs.8 a and b show the back and the front side of the array, respectively, which is incorporated with the L/X, L and L/S sub-arrays (from up to bottom in Fig.8a). The S-parameters were measured using the Agilent 8722ES and the measured radiation patterns were obtained in an anechoic chamber, while all the losses such as the insert losses of coaxial line, connectors and power dividers were compensated in the process.

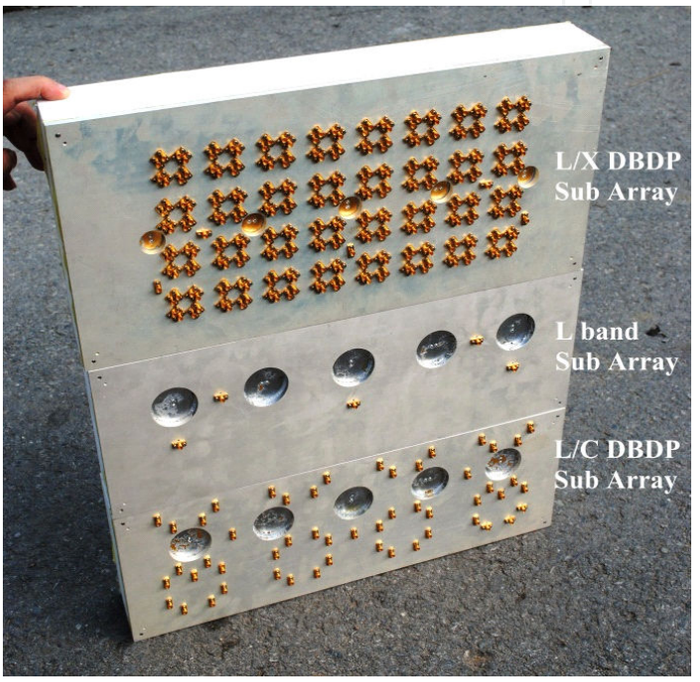

(a)

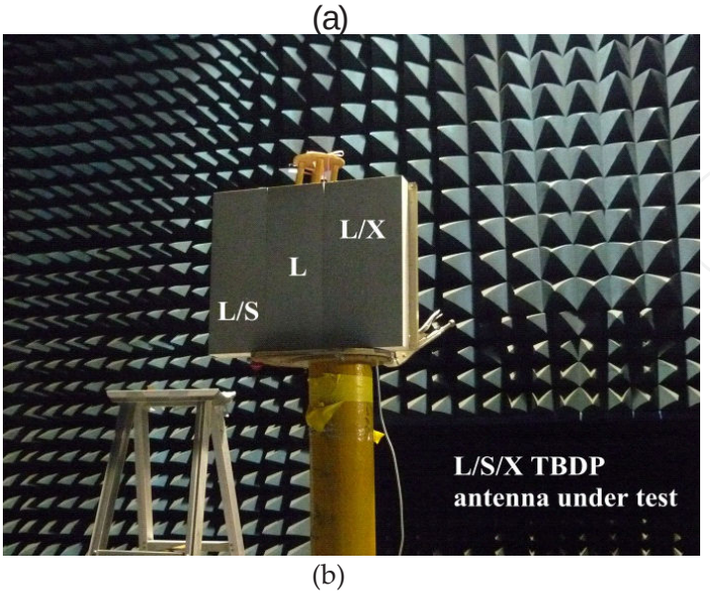

(b)

Figure 8. Photos of TBDP array

http://dx.doi.org/10.5772/54666

4.1. L-band

The measured L-band S_{11} and radiation patterns are shown in Fig.9 and Fig.10. It is seen that though the boundary conditions of L-band elements in L, L/S and L/X sub-arrays are quite different, similar return loss performance is measured except for LS4, which perhaps is caused by the solder false. The measured VSWR≤2 bandwidth is 167MHz (1.163-1.330GHz, 13.4%), and the array isolation is better than 37dB over the whole bandwidth (See Fig.9b). The array isolation hereinafter is defined as $-10\log_{10}|S_{21}|$, which is a positive dB value.

Although the whole L-band array is compounded by the elements in three separate sub-arrays, the measured radiation patterns keep in accordance with the theoretical ones, which means that the compound method raises little impact on the resulting radiation patterns. The cross-polarization level remains lower than -30 dB within the main lobe. The measured gain is 13.2dB (H-port) and 14.6dB (V-port), corresponding to the antenna efficiency of 62% and 61.2%, respectively. These lower figures may be related to its long electric-length of the microstrip and two-wire line feeder.

4.2. S-band

The narrowest VSWR≤2 bandwidth among all elements is defined as the array VSWR≤2 bandwidth. In S-band, an array VSWR≤2 bandwidth of 14.8% (3.25-3.768GHz) is measured according to Fig.11a, while the measured array isolation remains better than 45dB over the bandwidth (Fig.11b).

The measured radiation patterns agree well with the theoretical ones and the cross-polarization level keeps lower than -30dB in the main lobe (See Fig.12). Its measured front-back ratio is 37.8dB. The measured gain of 18.6dB is achieved for the 8×2 elements aperture, which means an antenna efficiency of 92.4%. Moreover, instead of the phase shifter, the coaxial line with custom-made length is applied to realize the scan experiment, as shown in Fig.13. From Fig. 14, a scan capability of ±27°is observed.

4.3. X-band

As shown in Fig.15, an array VSWR≤2 bandwidth of 16.8% (9.098- 10.781GHz) is measured in X-band with the array isolation better than -43dB over the whole bandwidth. From Fig.16, the measured radiation patterns fit well with the theoretical ones with the cross-polarization level better than -35dB in the main lobe. The measured front-back ratio is 42.3dB at the broadside direction, which is more than 4dB better than that of S band. It benefits from the larger electric size of the ground. Measured gains of 22.19dB (16×2 elements, V port) and 21.79dB (16×2 elements, H port) are realized, which mean the efficiencies of 92.7% and 84.5% at V- and H-ports, respectively. The scan radiation patterns of 30° in both ports and both planes were also measured. As shown in Fig. 17a-c,, the grate lobe of a little higher than -10dB appears around 80°-90°.

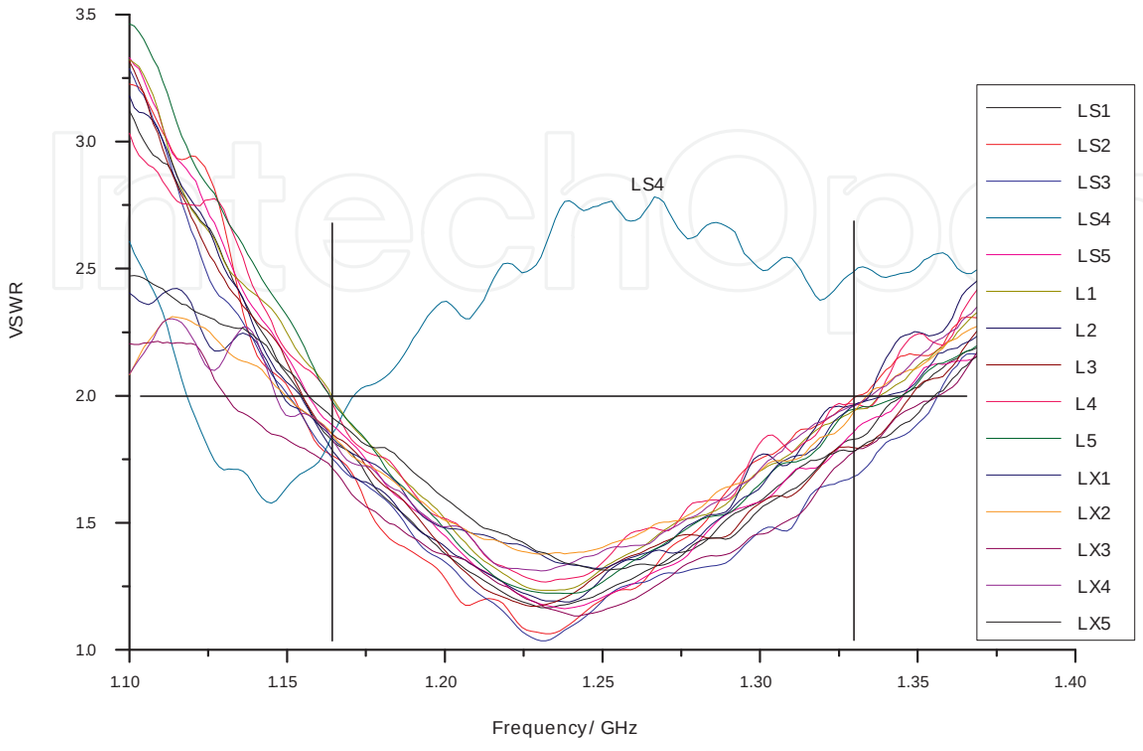

(a) VSWR of L-band elements (in L/S, L and L/X sub-arrays)

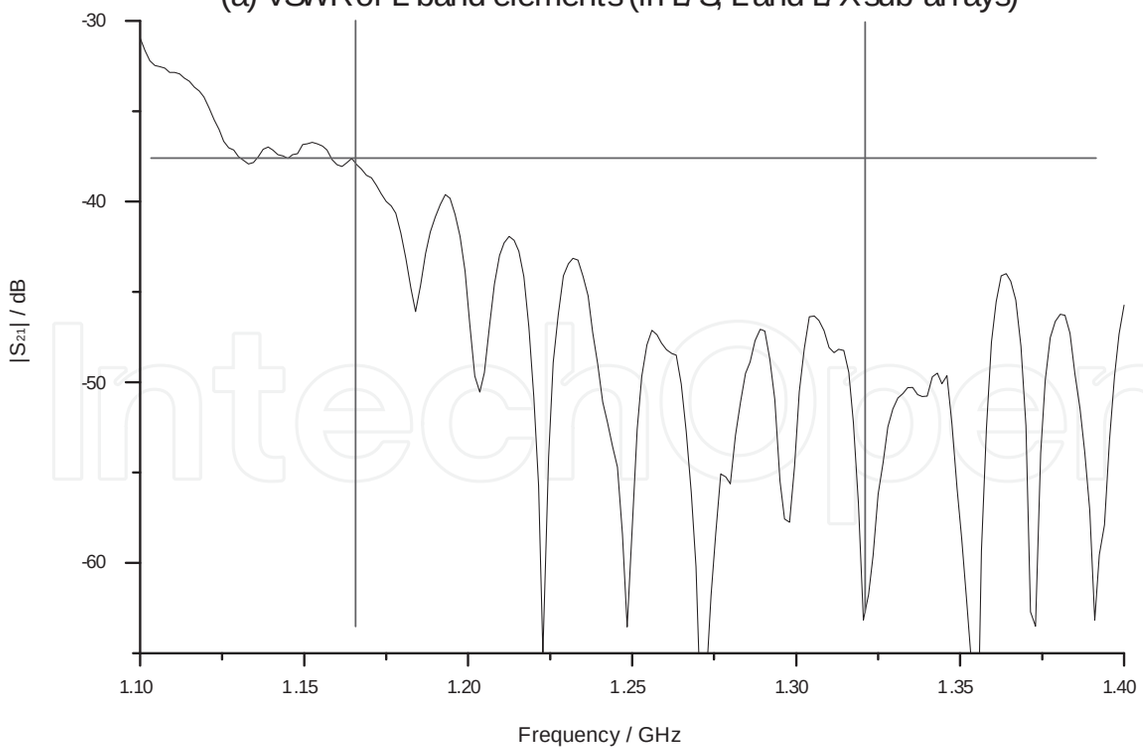

(b) Array isolation

Figure 9. Measured S parameters in L- band

http://dx.doi.org/10.5772/54666

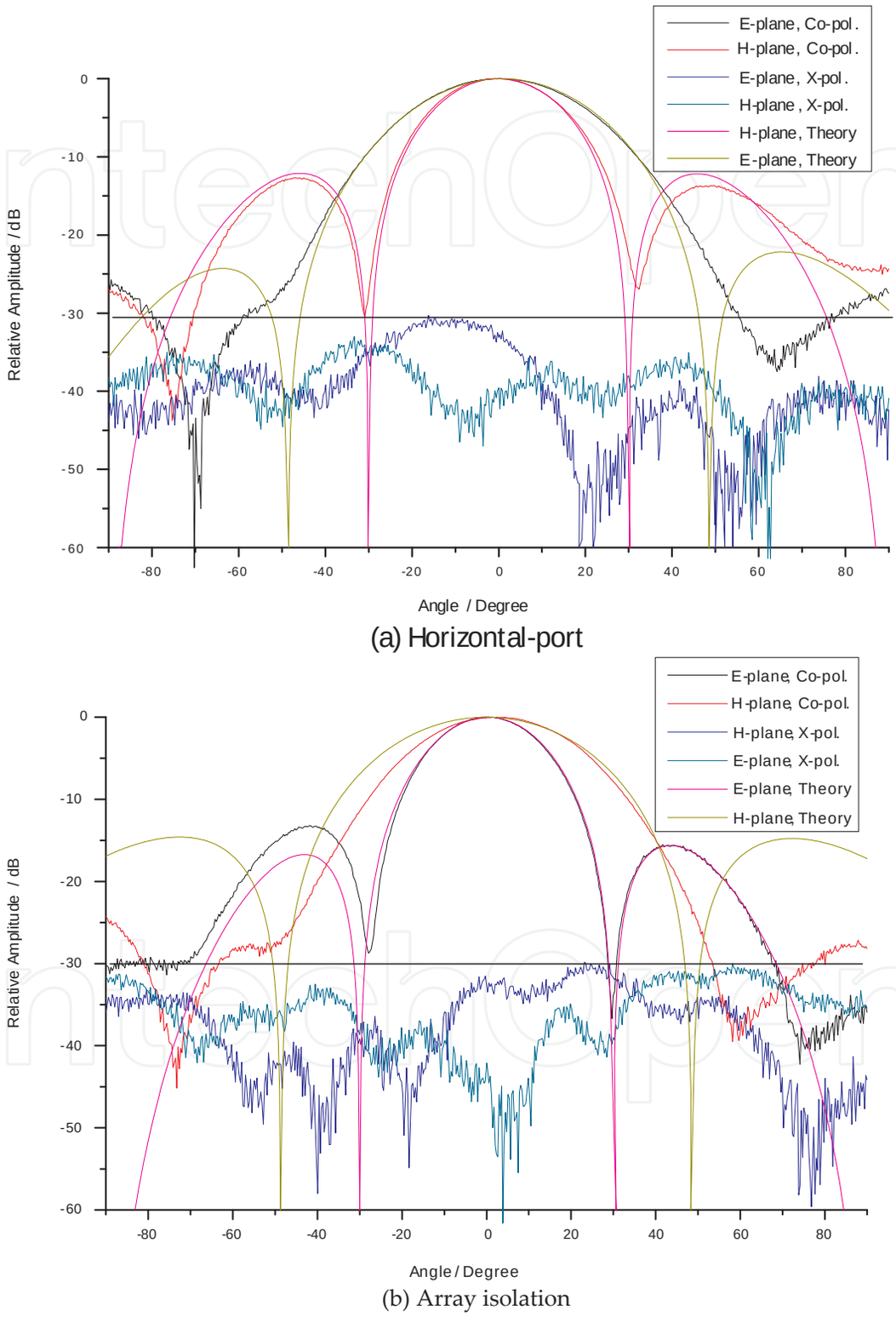

Figure 10. Measured and theoretical radiation patterns in L-band

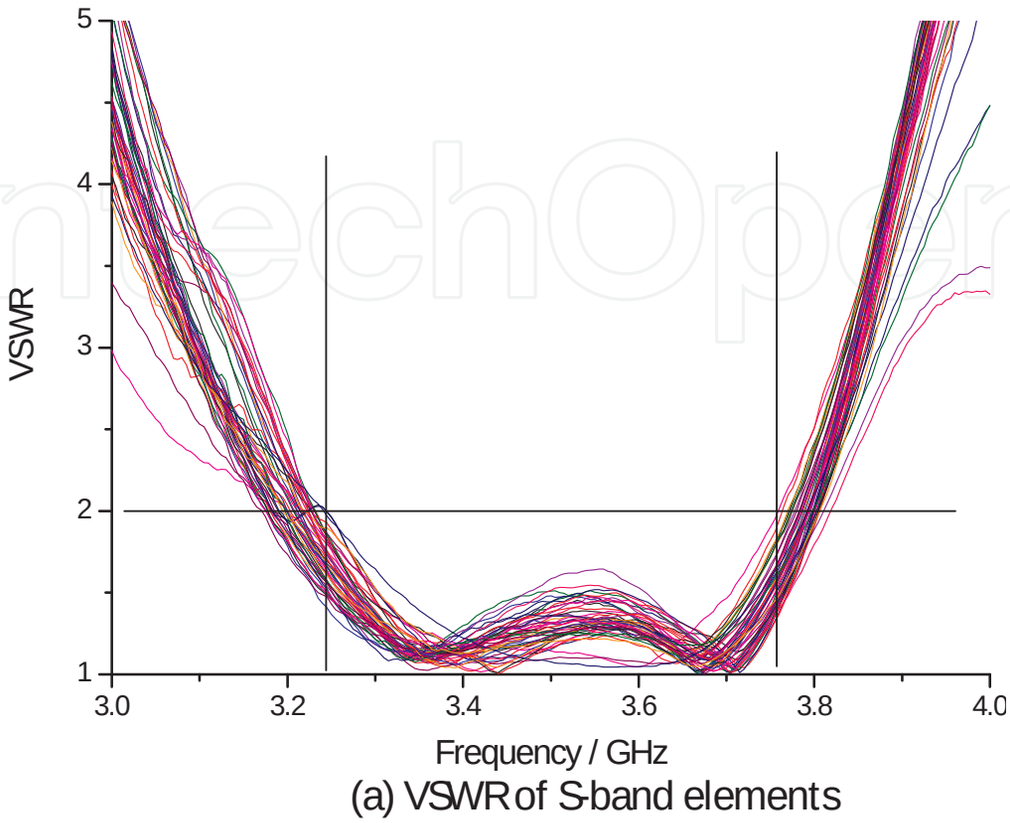

(a) VSWR of S-band elements

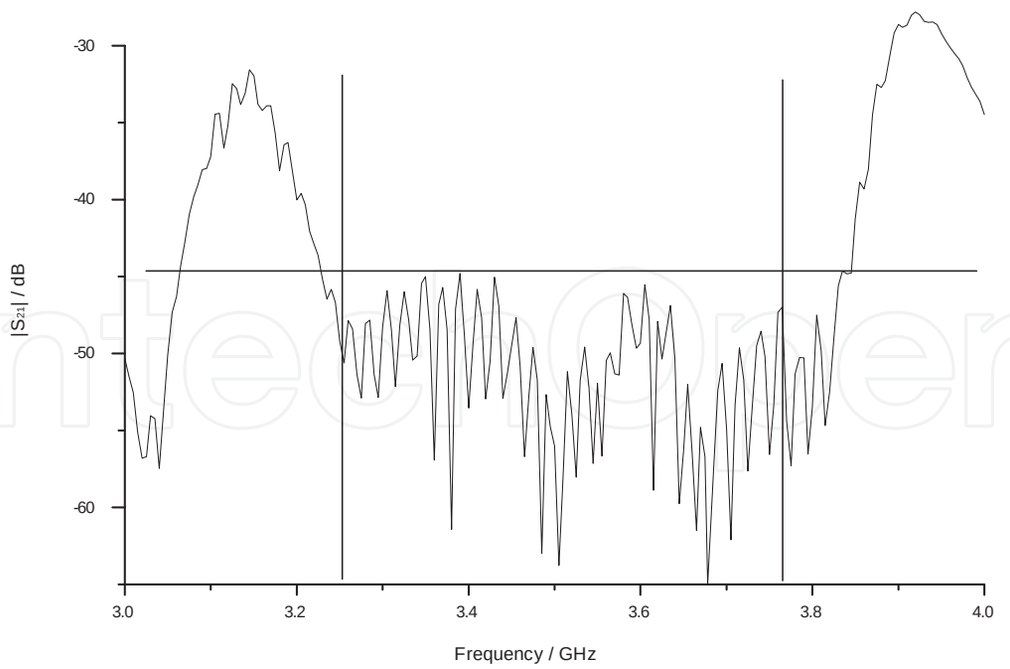

(b) Array isolation

Figure 11. Measured S parameters in S-band

http://dx.doi.org/10.5772/54666

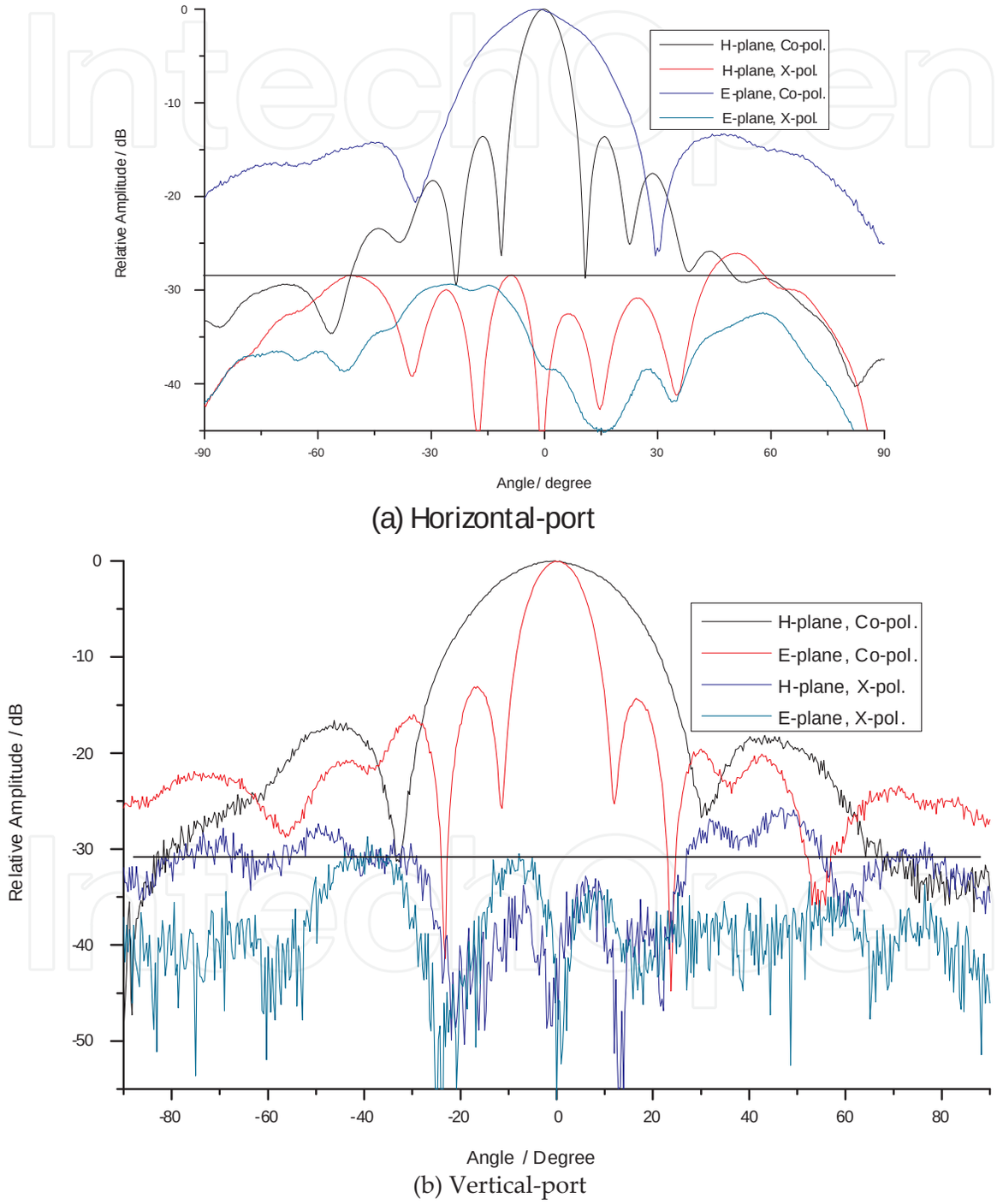

Figure 12. Measured radiation patterns in S-band

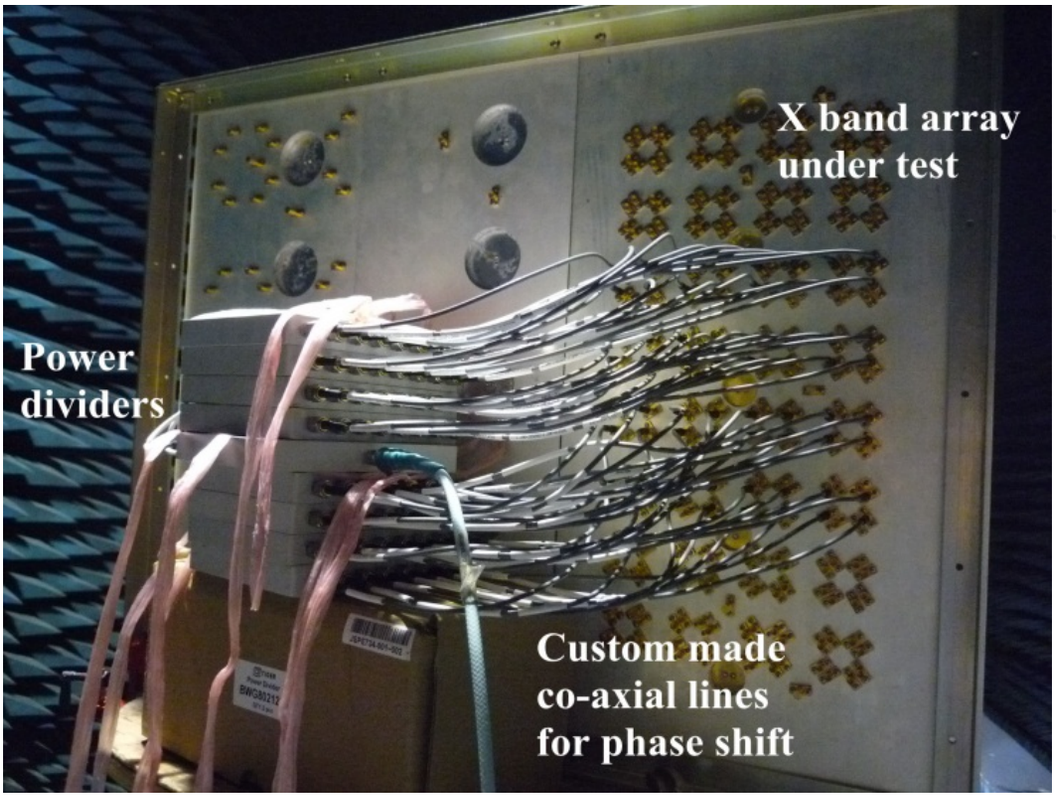

Figure 13. Custom-made coaxial lines instead of phase shifters

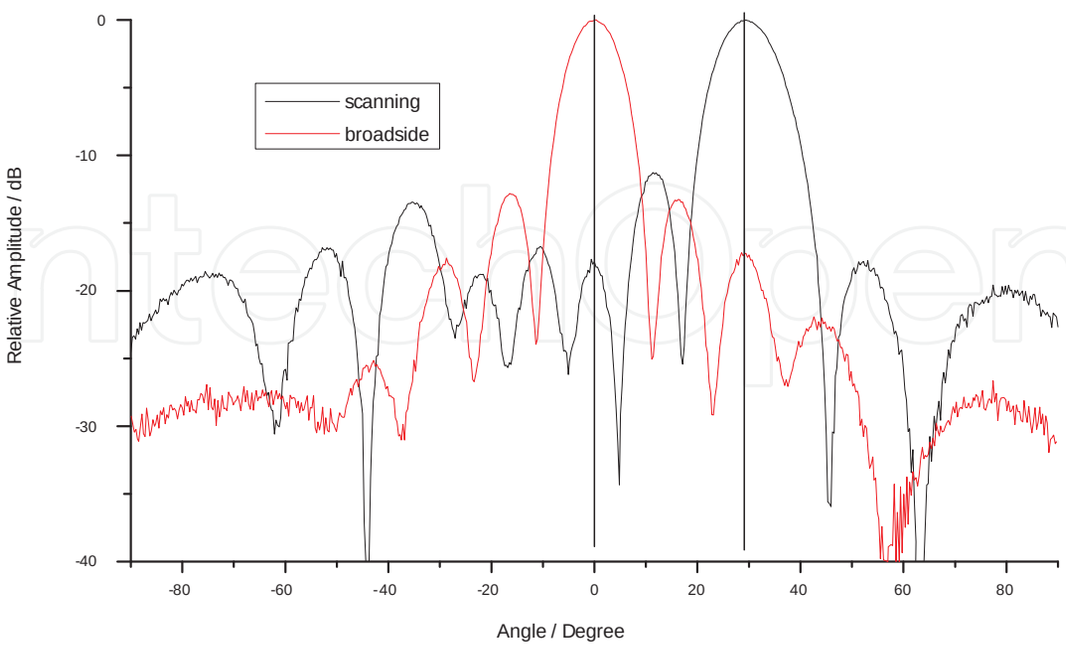

Figure 14. Scanning radiation patterns in S-band

http://dx.doi.org/10.5772/54666

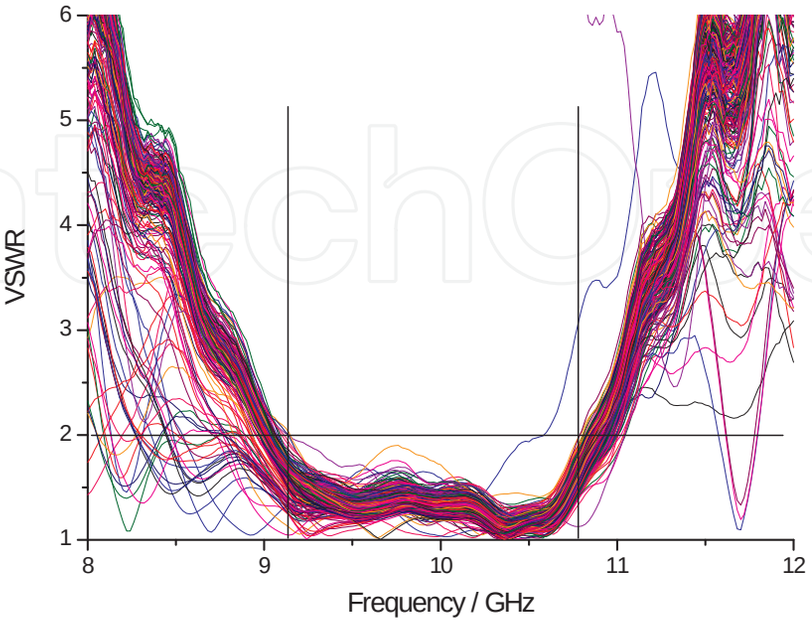

(a) VSWR of X-band elements

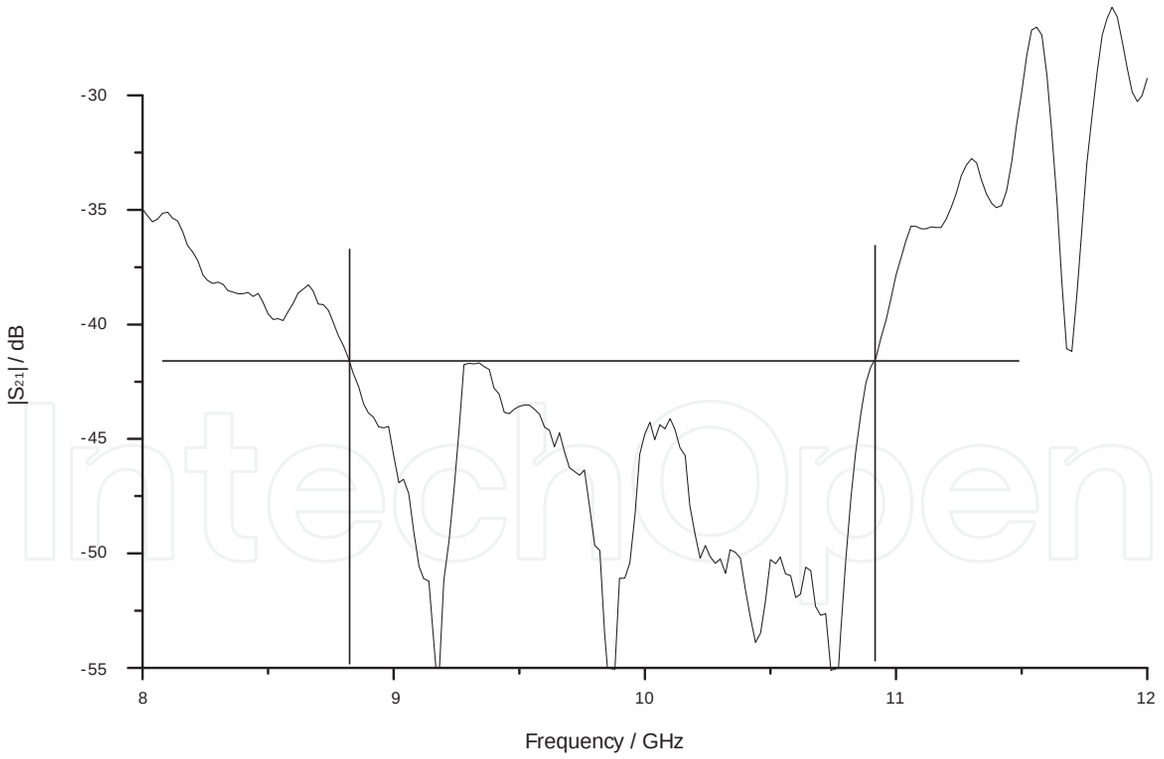

(b) Array isolation

Figure 15. Measured S-Parameters in X-band

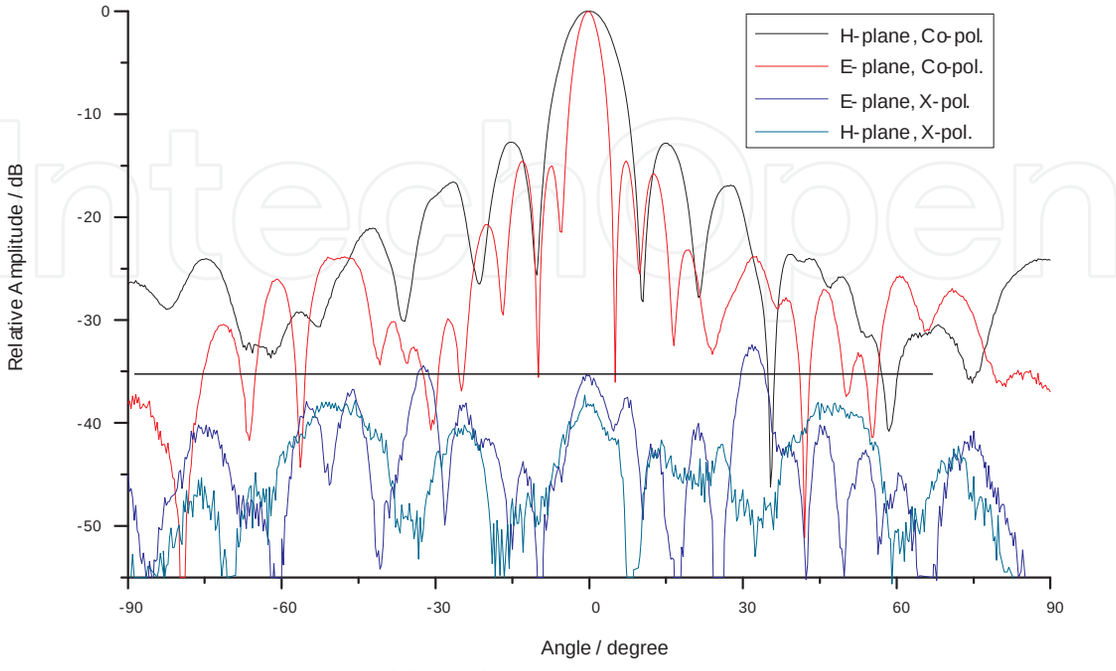

(a) Horizontal-port

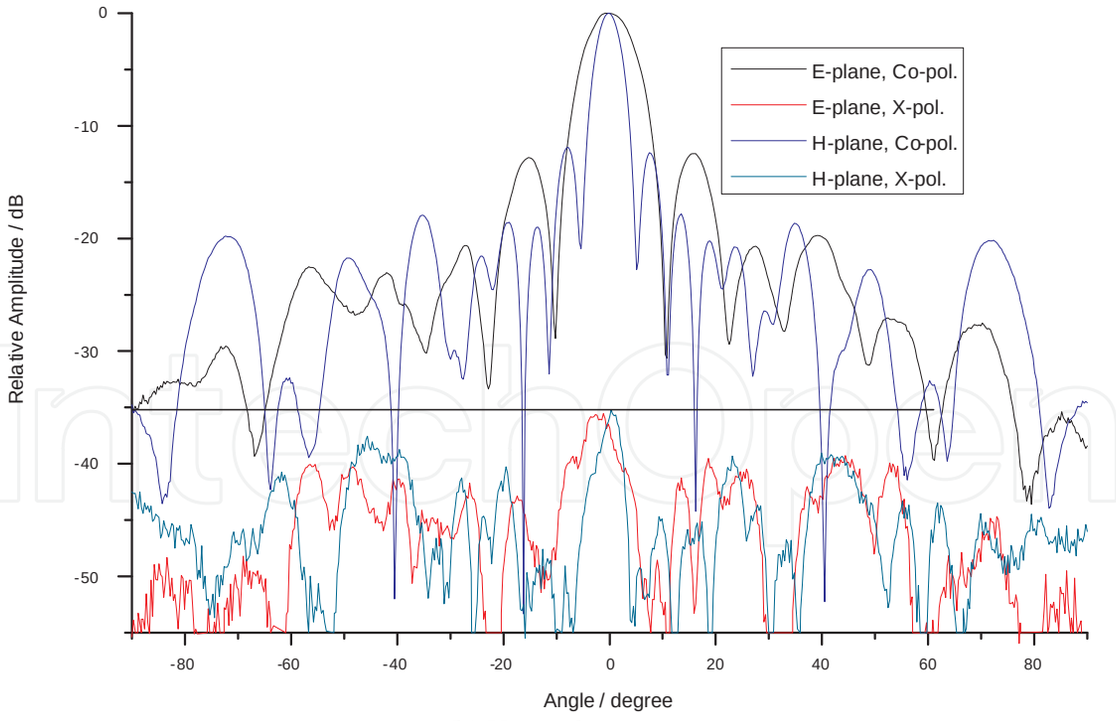

(b) Vertical-port

Figure 16. Measured radiation patterns and cross-polarization in X-band

http://dx.doi.org/10.5772/54666

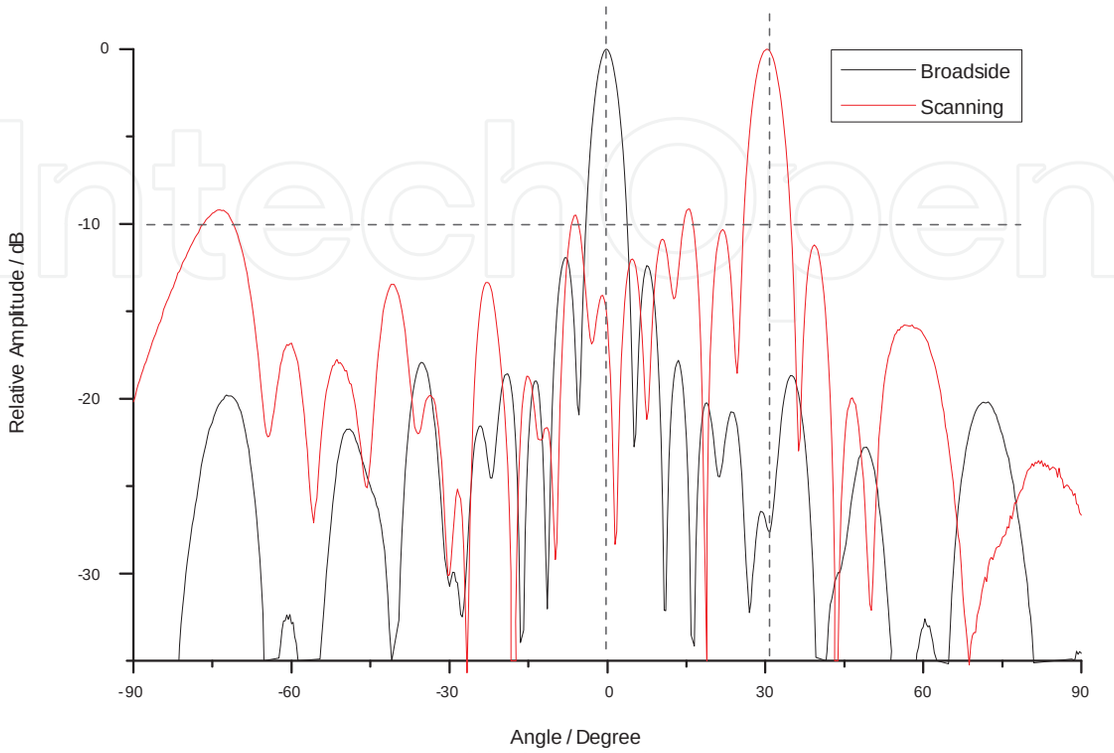

(a) H-pol. E-plane

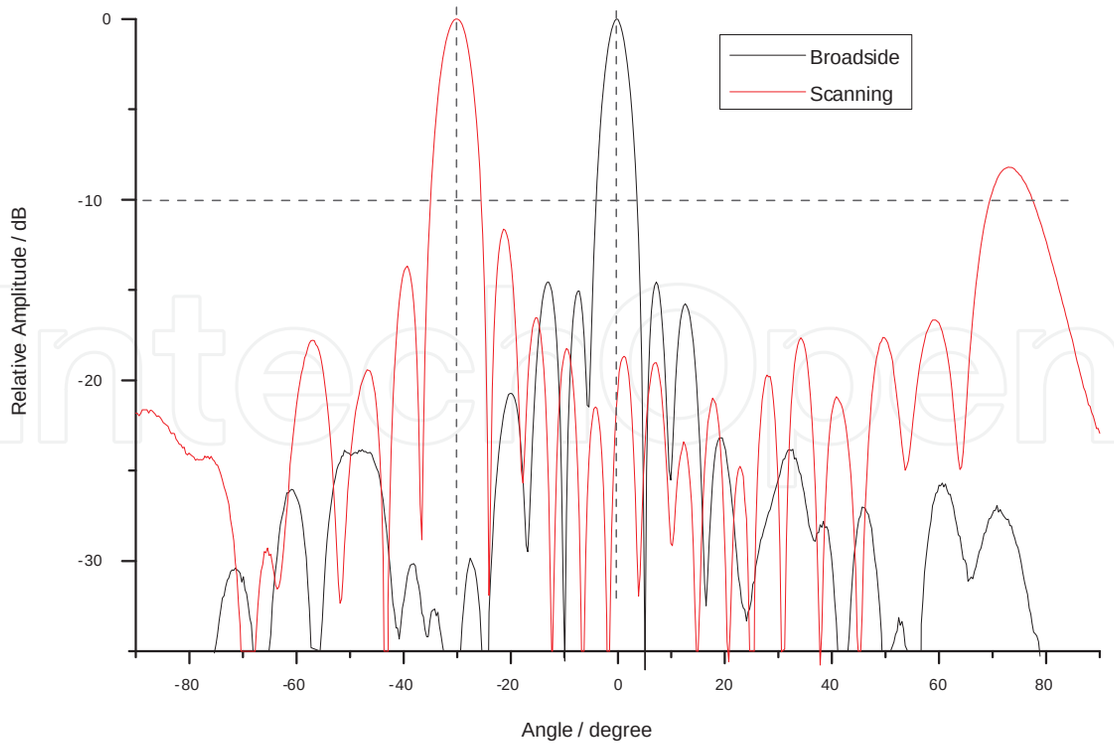

(b) V-pol. H-plane

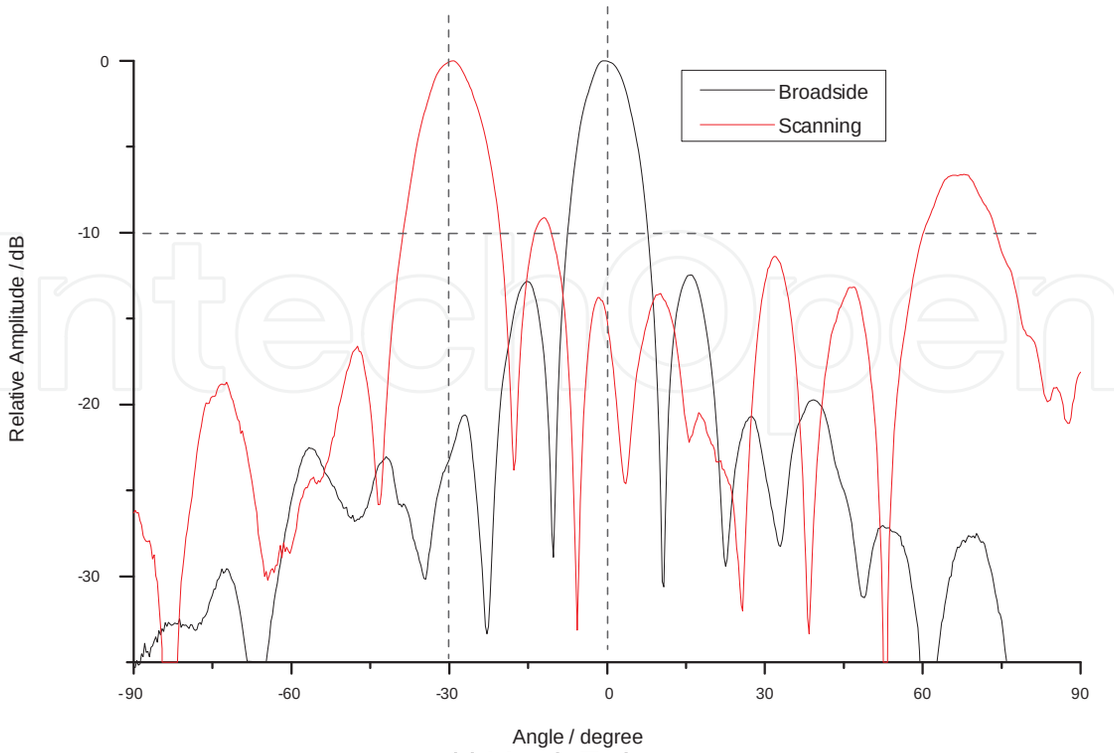

(c) V-pol. E-plane

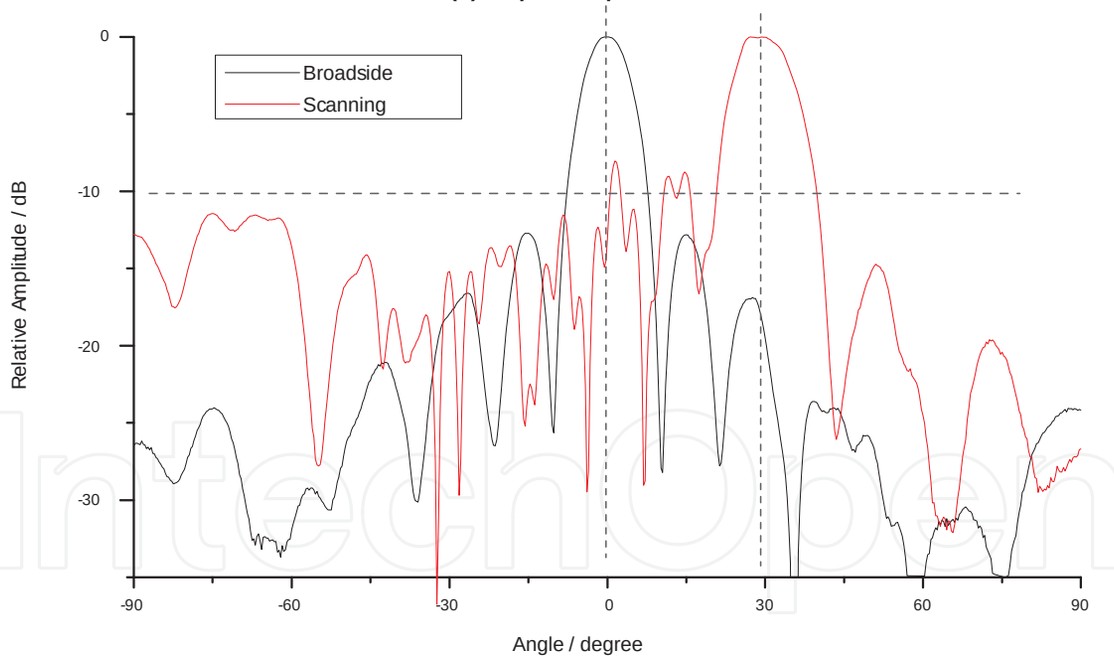

(d) H-pol. H-plane

Figure 17. Measured Scan Radiation Patterns in X-band

http://dx.doi.org/10.5772/54666

5. Conclusion

The method of assembling two DBDP shared-aperture sub-arrays and one single-band DP sub-array to form a MBDP shared-aperture array has been introduced. An array prototype has been fabricated and measured to validate the method. According to the measured results, the array prototype achieves satisfactory results: similar bandwidth of 13.4%~16.7% in three bands, the array isolation of better than 37dB for all bands and the cross-polarization level of lower than -30dB within the main lobe region and the scanning capacity of ±27 degree at S- and X- bands. The array prototype has a 33% off in the aperture size as compared with tri-band independent aperture antenna and exhibits robust characteristics throughout the bandwidths. This array design method can be extended to the shared-aperture arrays with more than three bands.

Acknowledgements

This work was supported by the National Nature Science Fund of China under Grants No. 60871030, No.61171031, and the National High-Technology Research and Development (863) Project of China under Grant No. 2007AA12Z125.

Author details

Shun-Shi Zhong and Zhu Sun

Shanghai University, China

References

[1] Jordan, R. L, Huneycutt, B. L, & Werne, M. "The SIR-C/X-SAR synthetic aperture radar system", IEEE Trans. on Geoscience and Remote Sensing, (1995). , 33(4), 829-839.

[2] Zhong, S..-S., "DBDP SAR Microstrip Array Technology", in Nasimuddin ed., Microstrip Antennas, InTech, Croatia, Chapter 17, (2011). , 433-452.

[3] Pozar,D. M.,and Targonski,S. D., "A shared-aperture dual-band dual-polarized microstrip array", IEEE Trans. Antennas Propagat., Feb. (2001). , 49(2), 150-157.

[4] Vetharatnam, G., Kuan, C. B., and Teik, C. H., "Combined feed network for a shared-aperture dual-band dual-polarized array", IEEE Antennas and Wireless Propagat. Letters, (2005). , 4, 297-299.

[5] Mangenot, C, & Lorenzo, J. "Dual band dual polarized radiating subarray for synthetic aperture radar", IEEE Antennas and Propagat. Society Int. Symp., (1999). , 3, 1640-1643.

[6] Hsu , S.-H., Ren, Y.-J., and Chang, K., "A dual-polarized planar- array antenna for S-band and X-band airborne applications", IEEE Trans. Antennas Propagat., Aug. (2009). , 51(4), 70-78.

[7] Soodmand, S., "A novel circular shaped dual-band dual-polarized patch antenna and Introducing a new approach for designing combined feed networks", 2009 Loughborough Antennas & Propagat. Conf., Loughborough, UK, Nov. (2009). , 401-404.

[8] Vallecchi, A, Gentili, G B, & Calamia, M. "Dual-band dual polarization microstrip antenna", IEEE Antennas and Propagat. Society Int. Symp.,, (2003). , 4, 134-137.

[9] Pozar, D. M, Schaubert, D. H, Targonski, S. D, & Zawadski, M. "A Dual-band dual-polarized array for spaceborne SAR", IEEE Antennas and Propagat. Society Int. Symp., Atlanta, GA, (1998). , 4, 2112-2115.

[10] Qu, X, Zhong, S. S, Zhang, Y. M, & Wang, W. "Design of an S/X dual-band dual-polarised microstrip antenna array for SAR applications", IET Microw. Antennas Propag., (2007). , 1(2), 513-517.

[11] Gao G. , Zhang, Y., Li, A., Zhao, J., &Cheng, H., "Shared-aperture Ku/Ka bands microstrip array feeds for parabolic cylindrical reflector", 2010 International Conference on Microwave and Millimeter Wave Technology (ICMMT),, (2010). , 1028-1030.

[12] Uher, R. P.J., & Pozar, D. M., "Dual-frequency and dual-polarization microstrip antennas for SAR applications", IEEE Trans. Antennas Propagat., Sept. (1998). , 46(9), 1289-1296.

[13] He , S. & Xie, J., "Analysis and design of a novel dual-band array antenna with a low profile for 2400/5800-MHz WLAN systems", IEEE Trans. Antennas Propagat., Feb. (2010). , 58(2), 391-396.

[14] Zhong, S.-S., Sun, Z., & Tang, X.-R., " Progress in dual-band dual polarization shared-aperture SAR antennas", Frontiers of Electrical and Electronic Engineering in China,Sept.(2009). (3), 323-329.

[15] Schippers, H, Verpoorte, J, Jorna, P, Hulzinga, A, Thain, A, Peres, G, & Van Gemeren, H. "Development of dual-frequency airborne satcom antenna with optical beamforming",, 2009 IEEE Aerospace conference, Big Sky, MT, March (2009).

[16] Li, P, Luk, K. M, & Lau, K. L. "A Dual-feed dual-band L-probe patch antenna", IEEE Trans. Antennas Propagat., July (2005). , 53(7), 2321-2323.

[17] Parker, G. S, Antar, Y. M. M, Ittipiboon, A, & Petosa, A. "A dual polarised microstrip ring antenna with good isolation", Electronics Letters, May (1998). , 34(11), 1043-1044.

[18] Gao, S.-C., Li, L.-W, Leong, M.-S, & Yeo, T.-S., "Dual-polarized slot-coupled planar antenna with wide bandwidth", IEEE Trans. Antennas Propagat., Mar. (2003). , 51(3), 441-448.

[19] Waterhouse, R. B. "Design of probe-fed stacked patches", IEEE Trans. Antennas Propagat., Dec. (1999). , 47(12), 1780-1784.

[20] Gao ,S. & Sambell, A., "Dual-polarized broad-band microstrip antennas fed by proximity coupling ", IEEE Trans. Antennas Propagat., Jan. (2005). , 53(1), 526-530.

[21] Wong H., Lau, K.-L. , & Luk, K.-M., "Design of dual-polarized L-probe patch antenna arrays with high isolation", IEEE Trans. Antennas Propagat., Jan. (2004). , 52(1), 45-52.

[22] Brachat, P, & Baracco, J. M. "Printed radiating element with two highly decoupled input ports", Electronics Letters, Feb. (1995). , 31(4), 245-246.

[23] Wong, K.-L., Tung, H.-C., & Chiou, T.-W., "Broadband dual-polarized aperture-coupled patch antennas with modified H-shaped coupling slots", IEEE Trans. Antennas Propagat., Feb. (2002). , 50(2), 188-191.

[24] Yamazaki, M, Rahardjo, E. T, & Haneishi, M. "Construction of a slot-coupled planar antenna for dual polarisation", Electronics Letters, Oct. (1994). , 30(22), 1814-1815.

[25] Guo, Y.-X., Luk, K.-M., & Lee, K.-F., "Broadband dual polarization patch element for cellular-phone base stations", IEEE Trans. Antennas Propagat., Feb. (2002). , 50(2), 251-253.

[26] Chiou, T.-W., & Wong, K.-L., "Broad-band Dual-polarized single microstrip patch antenna with high isolation and low cross polarization", IEEE Trans. Antennas Propagat., Mar. (2002). , 50(3), 399-401.

[27] Sun ,Zhu, Zhong, Shun-Shi, & Tang, Xiao-Rong, "C-Band dual-polarized stacked patch antenna with low cross-polarization and high isolation", EuCAP 2009, Berlin, German, March (2009).

[28] Wincza, K, Gruszczynski, S, & Grzegorz, J. "Integrated dual-band dual-polarized antenna element for SAR applications", 2009 IEEE Wireless and Microwave Technology Conference (WAMICON'09), Clearwater, FL, April (2009).

[29] Zhong, S.-S., Sun, Z., Kong, L.- B., Gao, C., Wang ,W., & Jin, M.-P., "Tri-Band Dual-Polarization Shared-Aperture Microstrip Array for SAR Applications", IEEE Trans. Antennas Propagat., Sep. (2012). , 60(9)

[30] Woelders , K., & Granholm, J., "Cross-polarization and sidelobe suppression in dual linear polarization antenna arrays", IEEE Trans. Antennas Propagat., Dec. (1997). , 45(12), 1727-1740.

[31] Uz Zaman, A., Manholm, L.,. &. Derneryd, A., "Dual polarised microstrip patch antenna with high port isolation", Electronics Letters, Sept. (2007). , 43(10), 551-552.

[32] Kong, L.-B., Zhong, S.-S., & Sun, Z., "Broadband microstrip element design of a DBDP shared-aperture SAR array", Microwave and Optical Technology Letters, Jan. (2012). , 54(1), 133-136.

IntechOpen